

LA-9075-MS

UC-66b

Issued: October 1981

**Lithology and Hydrothermal Alteration  
Determination from Well Logs  
for the Cerro Prieto Wells, Mexico**

Prepared for the Los Alamos National Laboratory

by

**Iraj Ershaghi\*  
Shahed Ghaemian\*  
Doddy Abdassah\***

**DISCLAIMER**


This book was prepared as an account of work sponsored by an agency of the United States Government. Neither the United States Government nor any agency thereof, nor any of their employees, makes any warranty, express or implied, or assumes any legal liability or responsibility for the accuracy, completeness, or usefulness of any information, apparatus, product, or process disclosed, or represents that its use would not infringe privately owned rights. Reference herein to any specific commercial product, process, or service by trade name, trademark, manufacturer, or otherwise, does not necessarily constitute or imply its endorsement, recommendation, or favoring by the United States Government or any agency thereof. The views and opinions of authors expressed herein do not necessarily state or reflect those of the United States Government or any agency thereof.

\*Department of Petroleum Engineering, University of Southern California, University Park, Los Angeles, CA 90007.

Under Contract 4-L20-2164K

July 1981

**Los Alamos** Los Alamos National Laboratory  
Los Alamos, New Mexico 87545

DISTRIBUTION OF THIS DOCUMENT IS UNLIMITED 

## **DISCLAIMER**

**This report was prepared as an account of work sponsored by an agency of the United States Government. Neither the United States Government nor any agency Thereof, nor any of their employees, makes any warranty, express or implied, or assumes any legal liability or responsibility for the accuracy, completeness, or usefulness of any information, apparatus, product, or process disclosed, or represents that its use would not infringe privately owned rights. Reference herein to any specific commercial product, process, or service by trade name, trademark, manufacturer, or otherwise does not necessarily constitute or imply its endorsement, recommendation, or favoring by the United States Government or any agency thereof. The views and opinions of authors expressed herein do not necessarily state or reflect those of the United States Government or any agency thereof.**

## **DISCLAIMER**

**Portions of this document may be illegible in electronic image products. Images are produced from the best available original document.**

## CONTENTS

ABBREVIATIONS AND SYMBOLS . . . . .	v
ABSTRACT. . . . .	1
I. INTRODUCTION. . . . .	1
II. GEOLOGICAL SETTING. . . . .	2
III. CLAY MINERAL EFFECTS ON WELL LOGS . . . . .	6
A. Resistivity and SP Logs . . . . .	6
B. Neutron and Density Logs. . . . .	10
IV. USE OF HISTOGRAMS AND SPIDERWEB DIAGRAMS. . . . .	13
V. ESTIMATION OF $Q_v$ -DEPTH PROFILE. . . . .	18
A. Procedure . . . . .	18
B. Application to the Cerro Prieto Wells . . . . .	19
VI. BEHAVIOR OF FOUR-ARM CALIPER AND DIPMETER . . . . .	21
VII. SUMMARY AND CONCLUSIONS . . . . .	22
ACKNOWLEDGMENTS . . . . .	27
REFERENCES. . . . .	27

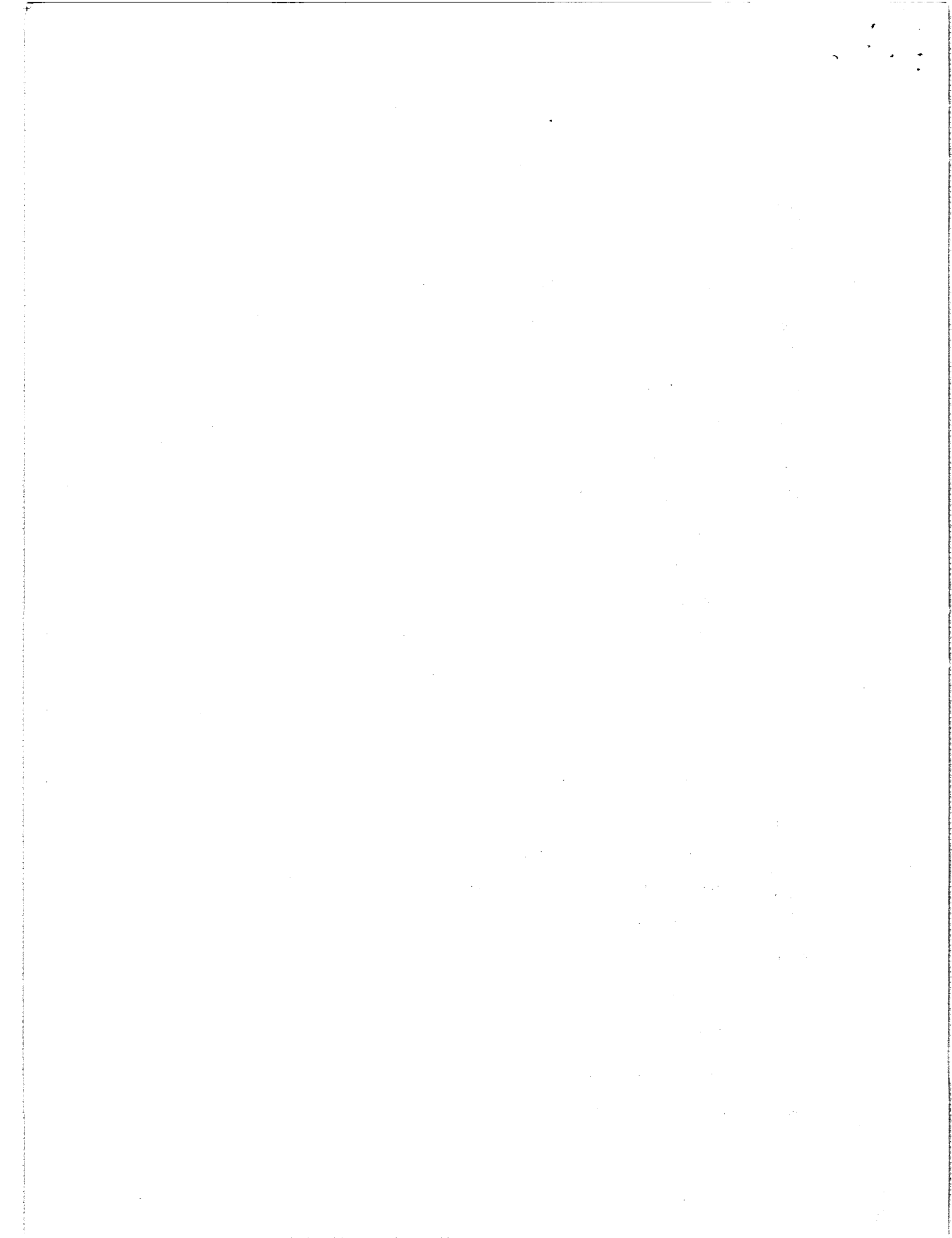
ABBREVIATIONS AND SYMBOLS

<u>Symbol</u>	<u>Definition</u>
a	Constant in equation $F = \frac{a}{\phi^m}$
B	Equivalent conductivity of the sodium concentrations, mho cm <sup>2</sup> /meq
C <sub>m</sub>	Electrical conductivity of brine at molal concentrations of m, mho/cm
C <sub>o</sub>	Electrical conductivity of the bulk formation, mho/cm
C <sub>w</sub>	Electrical conductivity of formation fluid, mho/cm
E <sub>m</sub>	Membrane potential, mv
E <sub>t</sub>	emf of cell with liquid junction, mv
F*	Formation resistivity factor of shaly sand
FDC	Compensated formation density
CNL	Compensated neutron log
K	(64.256 + .2394)T (in the SP equation)
m	Porosity exponent (cementation factor)
m <sub>1</sub>	Molal concentration of mud filtrate, mol/kg H <sub>2</sub> O
m <sub>2</sub>	Molal concentration of formation water, mol/kg H <sub>2</sub> O
Q <sub>v</sub>	Concentration of clay counter ions, meq/cm <sup>3</sup>
R <sub>w</sub>	Formation water resistivity ohm-m <sup>2</sup> /m
R <sub>mf</sub>	Mud filtrate resistivity, ohm-m <sup>2</sup> /m
SP	Spontaneous potential, mv
t <sub>Na</sub> <sup>h</sup>	Sodium Hittorf transport number
T	Temperature, °C

Greek

Subscripts

φ	Porosity	e	Equivalent
φ <sub>D</sub>	Density porosity	s	Sand
φ <sub>N</sub>	Neutron porosity	sh	Shale
φ <sub>S</sub>	Sonic porosity		



LITHOLOGY AND HYDROTHERMAL ALTERATION DETERMINATION  
FROM WELL LOGS FOR THE CERRO PRIETO WELLS, MEXICO

by

Iraj Ershaghi, Shahed Ghaemian,  
and Doddy Abdassah

ABSTRACT

The purpose of this study is to examine the characteristics of geophysical well logs against the sand-shale series of the sedimentary column of the Cerro Prieto Geothermal Field, Mexico. The study shows that the changes in mineralogy of the rocks because of hydrothermal alteration are not easily detectable on the existing logs. However, if the behavior of clay minerals alone is monitored, the onset of the hydrothermally altered zones may be estimated from the well logs.

The effective concentration of clay-exchange cations,  $Q_v$ , is computed using the data available from conventional well logs. Zones indicating the disappearance of low-temperature clays are considered hydrothermally altered formations with moderate- to high-permeability and temperature, and suitable for completion purposes.

---

I. INTRODUCTION

The basic objective in geothermal well logging is the detection of moderate- to high-permeability zones containing high-temperature fluids. Furthermore, identification of lithology and fluid composition will aid in regional mapping of the resource area.

Most geothermal systems are found in complex lithological units. To study such systems, one needs calibration data, which now are nonexistent. For simpler systems, such as sedimentary rocks, conventional well logs may have some application.

Consider a sand-shale series type of sediments that has been exposed to hydrothermal fluids (Fig. 1). Because of exposure to high temperatures and the

consequence of rock-fluid interaction, the properties of the rock may undergo severe alterations. The degree of such alteration is dependent upon the rock permeability. The higher the permeability, the more surface area is available to the invading hydrothermal fluids. Thus, the nature of alteration in permeable sand is expected to be different than that in the shales.

Hydrothermal alteration may result in the formation of microfractures. It may change the chemistry of the cementation material and various metamorphic reactions may take place, including dehydration and decarbonation.

To examine how these changes affect the well log response in a sedimentary-type geothermal field, a study was performed on the well logs from the Cerro Prieto field in Mexico.

A fair amount of well logs are available for the field. Copies of the logs were obtained through the Lawrence Berkeley Laboratory.

## II. GEOLOGICAL SETTING

The Cerro Prieto field is located on a plain in the Mexicali Imperial rift valley (Fig. 2). It covers  $29\,945 \times 10^3 \text{ m}^2$  (7400 acres). The geological setting consists of a thick high-temperature aquifer and an impermeable cap rock. The aquifer comprises 500-1000 m of permeable sandstone and conglomerate, interbedded with shale and siltstone. The cap rock consists of 400-700 m of shale, siltstone, and calcite cemented sandstone.

Elders et al.<sup>1</sup> reported on the x-ray diffraction analysis of samples from the Cerro Prieto wells. They reported on mineral assemblages associated with hydrothermal alteration in the area. Minerals corresponding to different levels of temperature were detected by these investigators. The mineralogical column consists of diagenetic minerals followed by moderate- to high-temperature minerals. From the data published by Elders et al, typical depth profiles may be plotted as seen in Figs. 3 to 6. Composition of the permeable beds with depth indicates significant changes in the types of clay minerals. Low-temperature clays disappear as deeper depths are reached. In high-temperature zones calc-aluminum silicates are a dominant feature. The low-temperature zones contain montmorillonite, dolomite, and ferric hydroxides. This is followed by the illite/chlorite zone in which the dolomite and ferric oxides disappear and montmorillonite and kaolinite are replaced by illite and chlorite. There is evidence of overgrowth and interstitial cementation in this zone. Below the



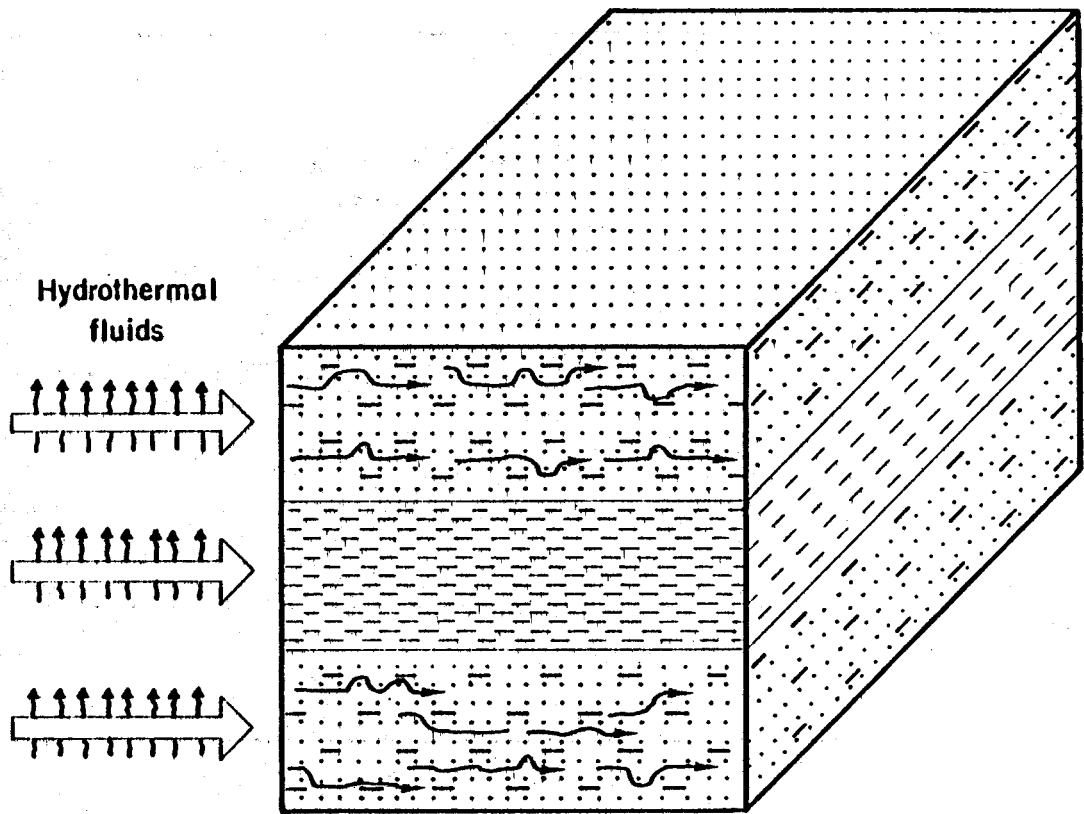


Fig. 1.

Sand-shale section exposed to hydrothermal fields.

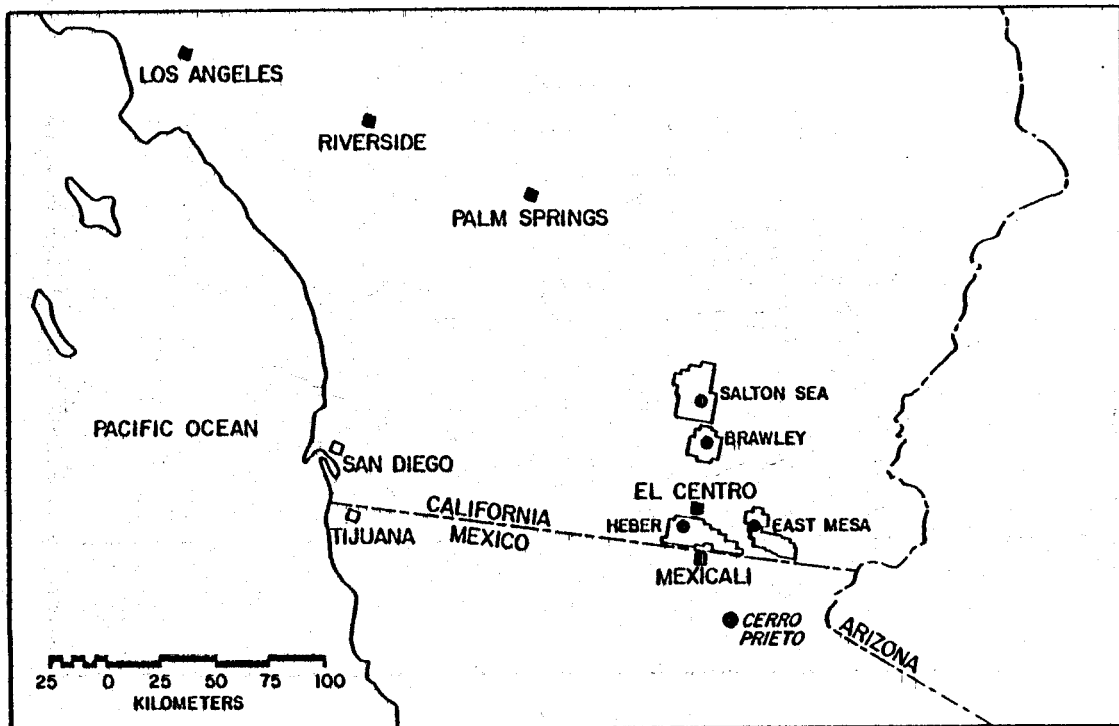


Fig. 2.

Geographical location of the Cerro Prieto field.

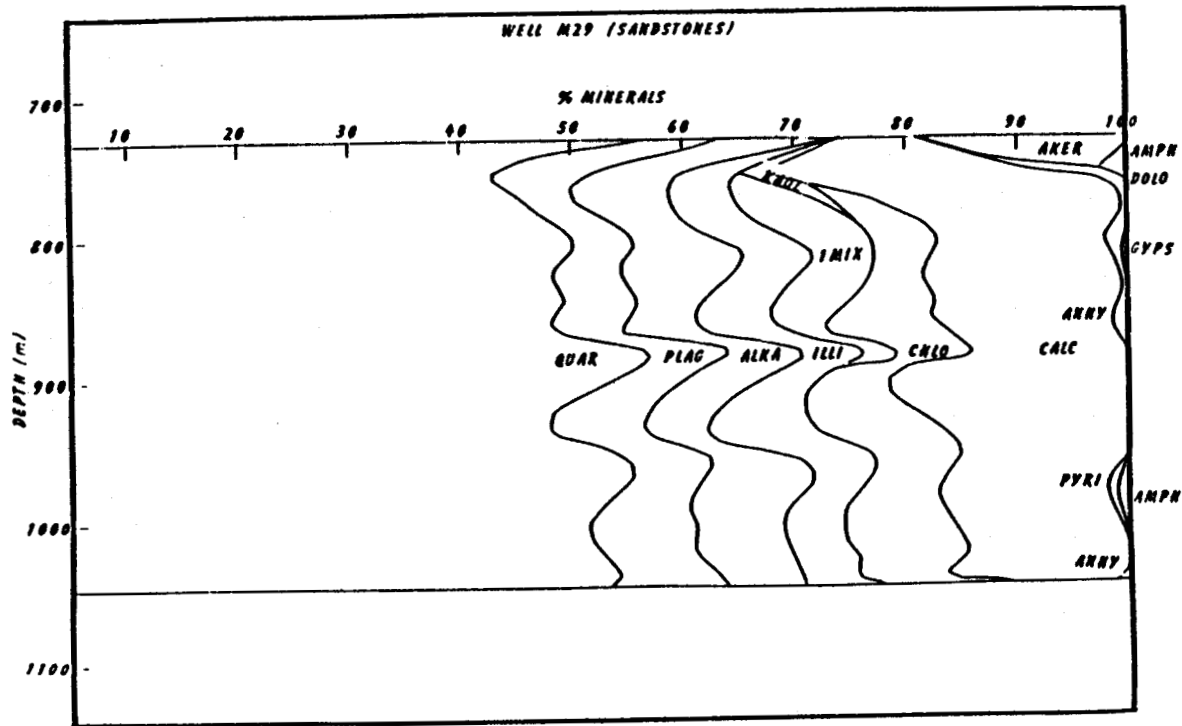


Fig. 3.

Mineralogical changes in sandstone, Well M-29.

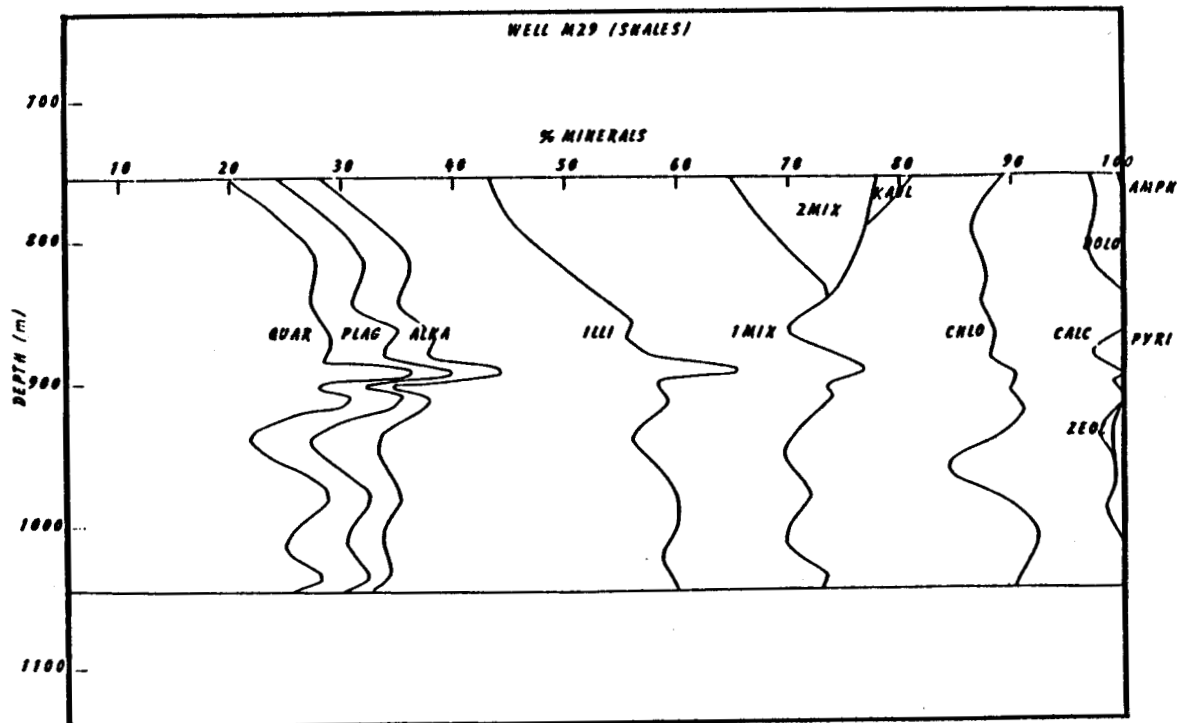


Fig. 4.

Mineralogical changes in shales, Well M-29.

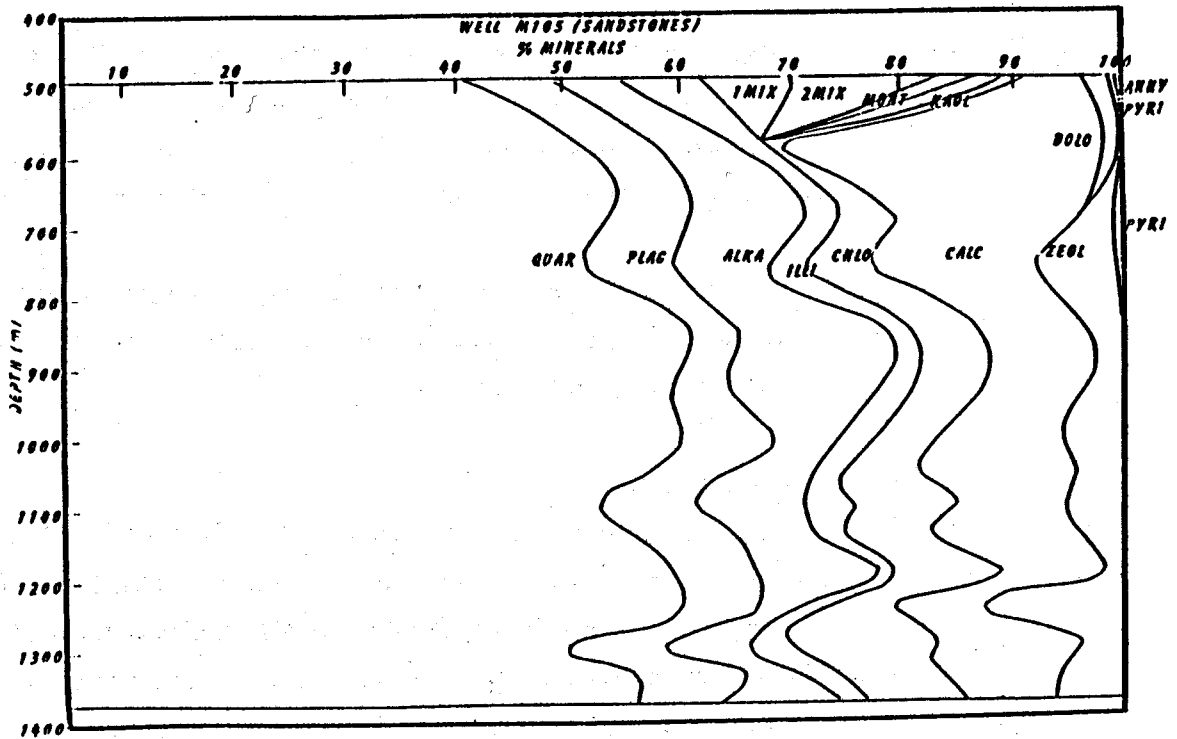


Fig. 5.

Mineralogical changes in sandstones, Well M-105.

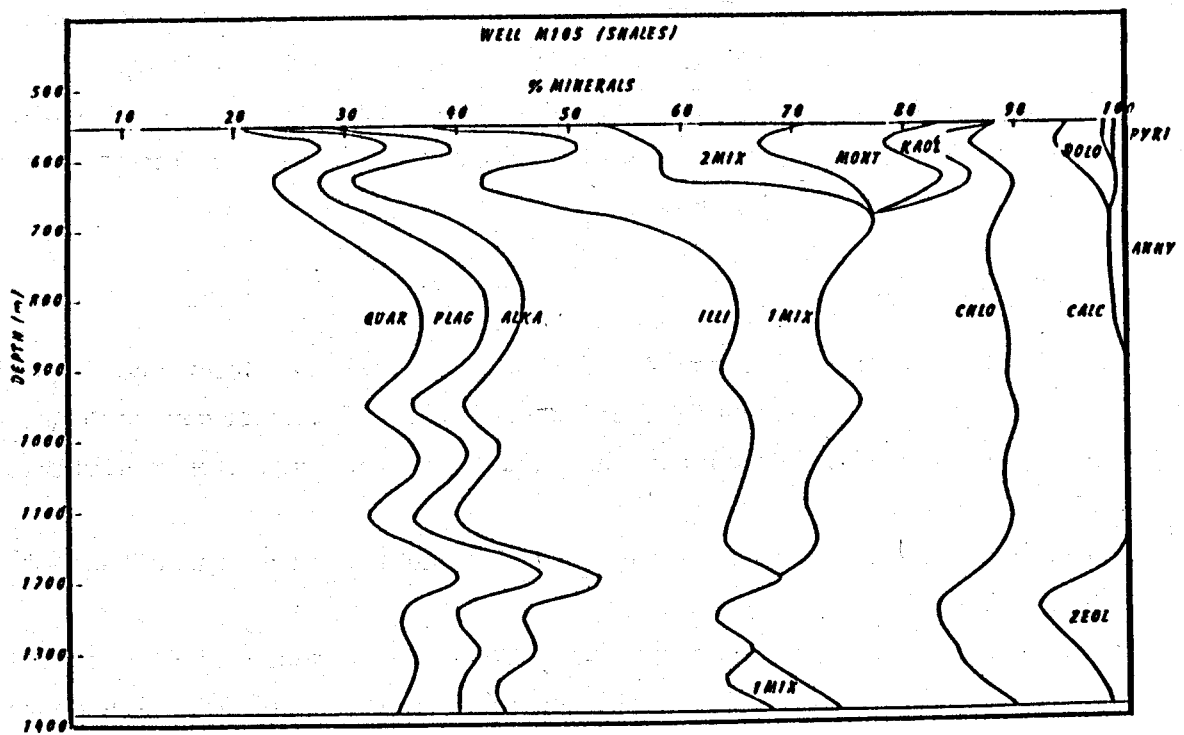


Fig. 6.

Mineralogical changes in shales, Well M-105.

illite/chlorite zone the hydrothermally altered zone is detectable from the presence of calc-aluminum silicates. Further manifestations of this zone are the disappearance of calcite, significant reduction in the concentration of illite, sulfide and wairakite, and the gradual appearance of prehnite, actinolite, diopside, and biotite.

Study of mineral composition in shales indicates similar changes. But, according to Elders et al.<sup>1</sup>, such changes in shales are noticeable at greater depth and higher temperatures than in sandstones.

### III. CLAY MINERAL EFFECTS ON WELL LOGS

In terms of affecting the well log responses, clay minerals may be classified effective and ineffective.<sup>2</sup> Effective clays such as montmorillonite and illite have high cation exchange capacity that gives rise to surface conduction and an overall lowering of formation electrical resistivity. Furthermore, these expandable clays have high hydrogen indices affecting the responses on neutron logs.

#### A. Resistivity and SP Logs

A careful review of the Dual-Induction Laterologs or Induction-Electric Surveys indicates a lowering of formation electrical conductivity with depth (Fig. 7). Correlation of these low conductivity zones with well completion data indicates that such zones are potential producers. Because of the shaliness of the producing sands, the electrical conductivity of the formation may be represented by the following model:<sup>3</sup>

$$C_o = \frac{1}{F^*} (C_w + BQ_v) \quad (1)$$

$C_o$  and  $C_w$  are the electrical conductivities of the bulk formation and formation fluid, respectively.  $B$  is the equivalent conductivity of sodium counterions,  $Q_v$  is the concentration of clay counterions, and  $F^*$  is the formation resistivity factor of shaly sand.

To examine the causes of lowering of  $C_o$ , we must examine the effect of each of the above elements.

A reduction in formation porosity will cause an increase in  $F^*$  and will contribute to the lowering of  $C_o$ . Evidence of porosity reduction with depth is quite clear from existing porosity logs. If one assumes that porosity reduction is the sole cause for the lowering of  $C_o$ , and that  $C_w$  and  $BQ_v$  are constant

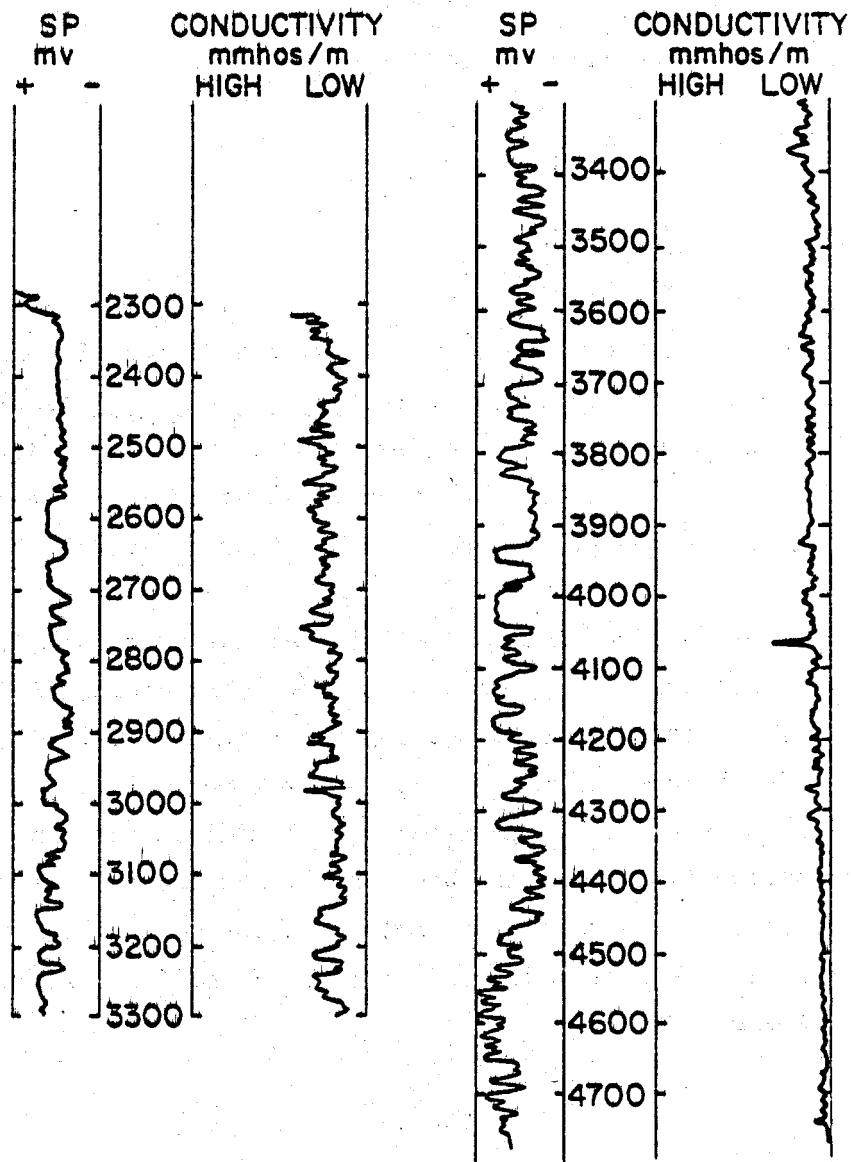


Fig. 7.

Typical reduction of electrical conductivity with depth, Well M-19.

throughout the geologic column, then the following must be true:

$$\frac{(C_o)_{\text{shallow}}}{(C_o)_{\text{deep}}} = \frac{(F^*)_{\text{deep}}}{(F^*)_{\text{shallow}}} = \frac{(a/\phi^m)_{\text{deep}}}{(a/\phi^m)_{\text{shallow}}} \quad (2)$$

Assuming similar a's and m's:

$$\frac{(C_o)_{\text{shallow}}}{(C_o)_{\text{deep}}} = \left( \frac{\phi_{\text{shallow}}}{\phi_{\text{deep}}} \right)^m \quad (3)$$

Shallow porosities are in the range of 0.30+ and deep porosities are in the range of 0.22+. This means the ratio of  $(C_o)_{\text{shallow}}/(C_o)_{\text{deep}}$  should be in the range of 2 to 1. An examination of the deep conductivity log indicates that the lowering of conductivities are more than a factor of 2. (See Table I.) Thus, in addition to the change in porosities, either  $C_w$  and/or  $BQ_v$  must be changing with depth.

To cause a lowering of  $C_o$  the conductivity of the formation fluid  $C_w$  must decrease. This is unlikely. The total dissolved solid concentration is expected to be high in potentially producing zones that have been exposed to hydrothermal fluids, because of rock fluid interactions. Furthermore, the existence of high temperatures in such zones will tend to increase  $C_w$ . A reduction in formation fluid salinity with depth, for the same type of mud filtrate, will tend to decrease the deflection of the spontaneous potential (SP). Examination of the logs indicates that the SP deflections increase in hydrothermally altered zones.

TABLE I

TYPICAL ELECTRICAL CONDUCTIVITY CHANGES WITH DEPTH

Well	Depth Range (m)	Average Conductivity
19	762	1000
	1524	200
21	533	900
	1295	350
14	838	1000
	1200	350

The only other factor left is the contribution of the  $BQ_v$  term. Variations of B with formation fluid salinity is negligible. Table II shows the estimated B values for a salinity range from 5000 to 30000 ppm.

To relate the changes in  $Q_v$  to the observed increases in formation electrical conductivity and the spontaneous potential, the following discussion on cation exchange capacity of clays and its influence on well log responses is in order.

Clays are inorganic polyelectrolytes of aluminum silicate hydrates. All natural occurring clays are negatively charged. Density of the negative charges can be measured by determining the number of positive charges that are required to neutralize the crystal. This is known as the cation exchange capacity (CEC) of the clay and is expressed in milliequivalents per 100 grams of clay.

Clays may be classified as swelling or nonswelling. Montmorillonite is the only clay that swells by adsorbing ordered layers of water between the clay crystals. This is due to hydration of the cation attracted to the clay and hydrogen bonding.

Mixed layered clays which contain montmorillonite will also swell with water, but the illite portion is relatively nonwater swelling. Kaolinite, chlorite, and illite may be classified as nonwater swelling. They do, however, absorb some water.

Clay surfaces, dispersed in porous rock containing a brine solution, can conduct electricity. The contribution of surface conductivity to overall rock conductivity has been discussed by Uco<sup>4</sup> and Waxman and Smits.<sup>3</sup>

TABLE II  
VARIATION OF B WITH SALINITY AT 25°C

Salinity (ppm)	B, mho cm <sup>2</sup> /meq
10000	0.038
20000	0.0438
30000	0.0450
40000	0.046
50000	0.046

Hill and Milburn<sup>5</sup> showed a relationship between  $Q_v$  and the membrane potential of a shaly sand core plug in an electrochemical cell. Subsequent work by Smits<sup>6</sup> and Thomas<sup>7</sup> showed the influence of  $Q_v$  on spontaneous potentials measured in boreholes.

As shown by Smits, the electrochemical potential developed in shaly sands can be estimated from the difference between  $(E_m)_{sh}$  and  $(E_m)_s$ .

$$(E_m)_{sh} = \int_{m_1}^{m_2} \frac{C_m + [(B)C_m \cdot Q_v]_{sh} / t_{Na}^h}{C_m + [(B)C_m \cdot Q_v]_{sh}} \cdot \frac{dEt}{dm} \cdot dm \quad (4)$$

$$(E_m)_s = \int_{m_1}^{m_2} \frac{C_m + [(B)C_m \cdot Q_v]_s / t_{Na}^h}{C_m + [(B)C_m \cdot Q_v]_s} \cdot \frac{dEt}{dm} \cdot dm \quad (5)$$

Explanation for the terms is given in the nomenclature. From these equations it is seen that, as the  $Q_v$  of the clay particles in a shaly sand increases,  $(E_m)_s$  will increase and the overall SP deflection becomes small. This is the so-called "shaly sand" response on SP logs. One cautionary note here is to recognize that in addition to the changes in  $Q_v$ , variations in  $R_{mf}/R_w$  ratio will also affect the SP readings. Thus, in the above discussion on  $Q_v$  it is assumed that  $R_{mf}/R_w$  ratio is unchanged.

From this discussion, it is quite clear that under a given set of formation fluid salinity and mud filtrate salinity, the exact nature of interstitial clays, as determined by  $Q_v$ , will have significant effect on both formation conductivity and the SP log.

#### B. Neutron and Density Logs

Overlays of compensated neutron log and compensated density log porosities may be used to detect the presence of clays in the formation. In the unaltered sections of the wells in the Cerro Prieto field, such overlays clearly show the presence and the contribution of clays ( $\phi_N < \phi_D$ ). Figure 8 is an example for Well M-42. For the same well and against a hydrothermally altered zone, a reversal ( $\phi_N < \phi_D$ ) in the relative portion of the two porosity logs occurs (Fig. 9). Such reversals may be indicative of low-hydrogen indices and/or temperature effects. No temperature corrections were made to the neutron



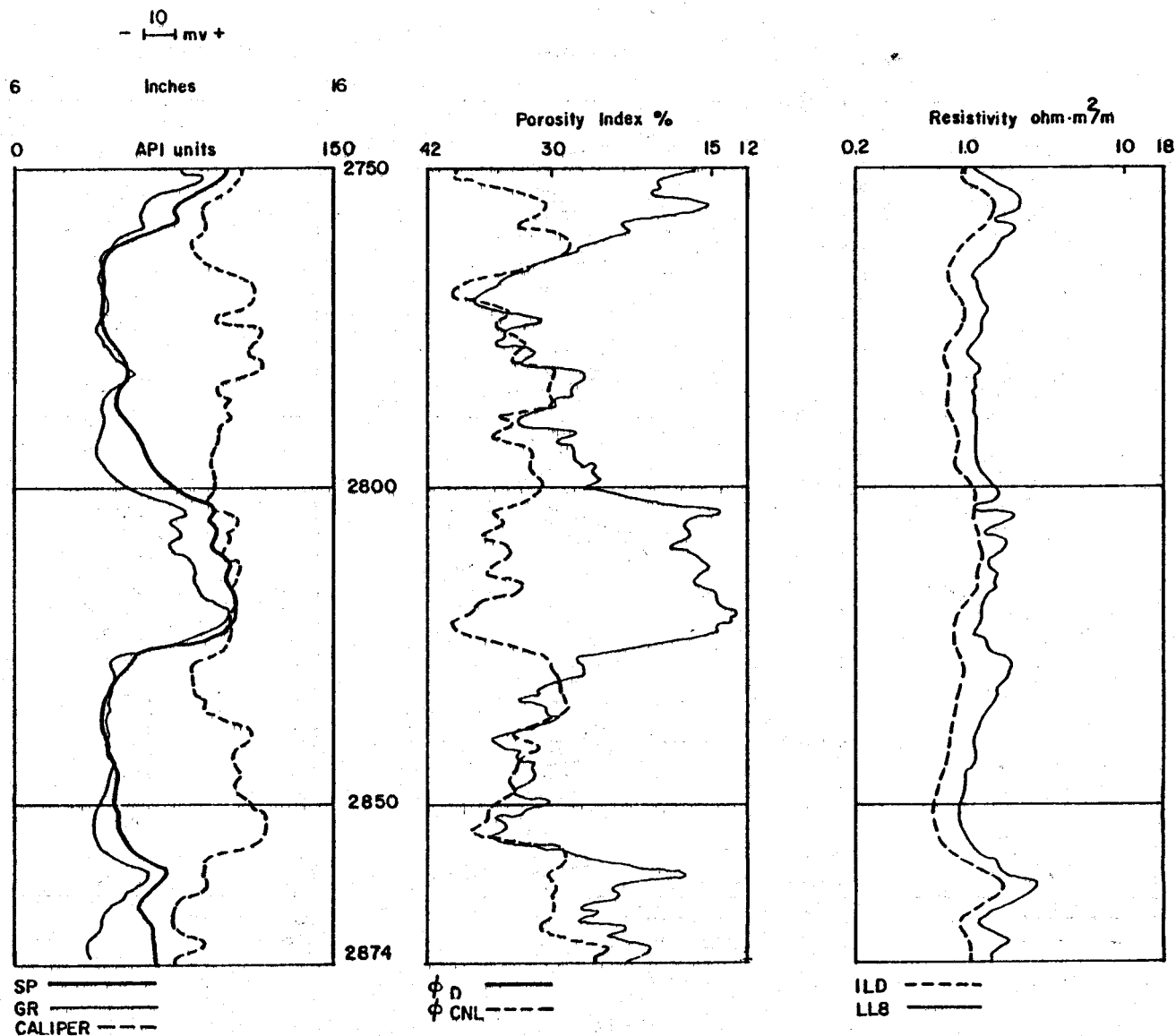


Fig. 8.  
Behavior of CNL and FDC in unaltered section of Well M-42.

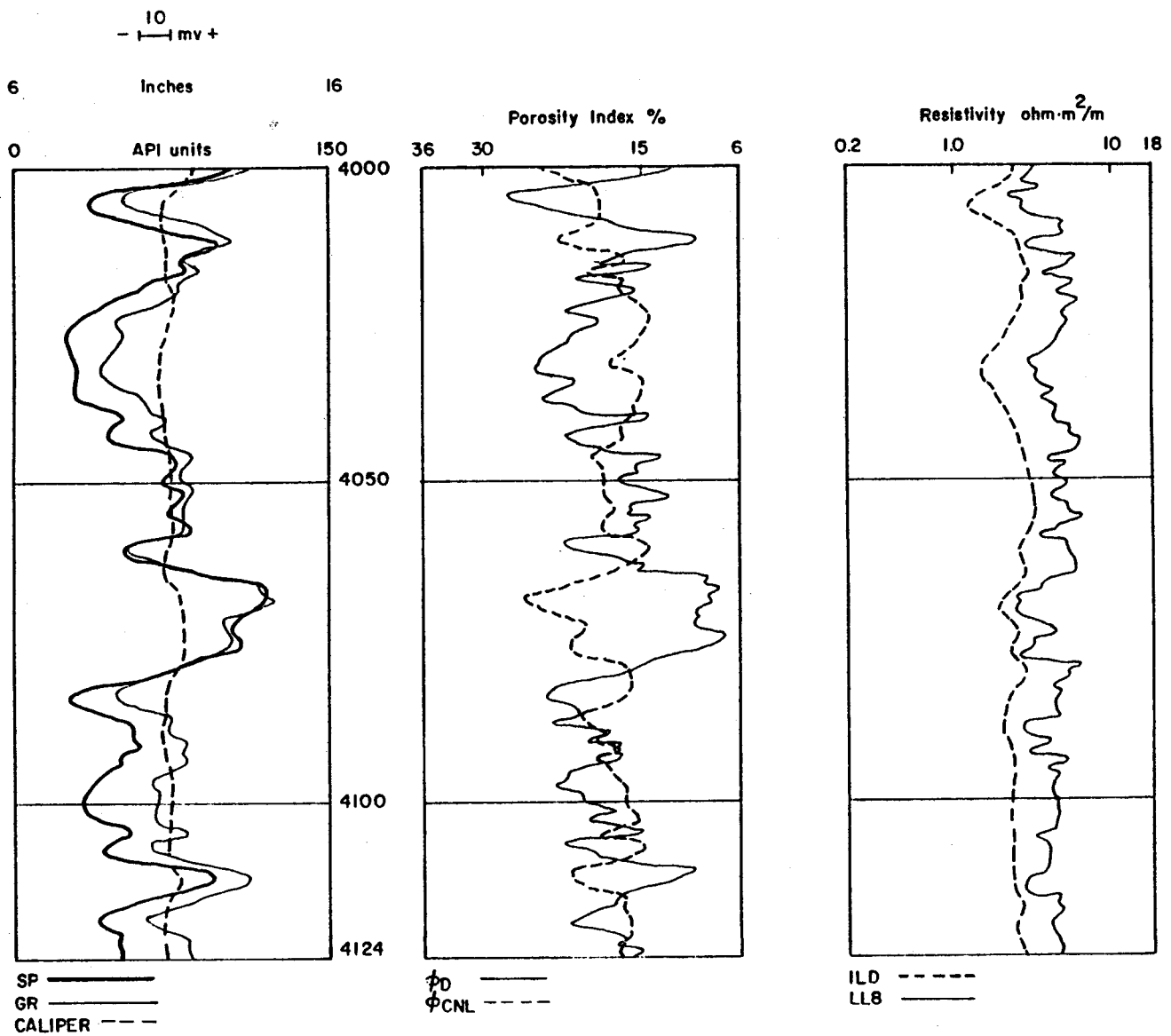


Fig. 9.  
Behavior of CNL and FDC in altered section of Well M-42.

porosities. Because no accurate estimate of reservoir temperature is available, current estimates are somewhat beyond the range of temperatures covered by existing charts. Indications are, however, that the temperature correction will result in an increase in the recorded  $\phi_N$  values by one or two porosity units.

To close the gap, corrections for both the low-hydrogen index and possible gas saturation must be applied. To examine the relative effect of these corrections, one must study the  $\phi_N$  vs  $\phi_D$  relationship in shales adjacent to the sands. As shown in Fig. 8, in the unaltered section of the well [856-862 m (2810-2830 ft)], the differential porosity is about 20 porosity units. The differential porosity in shales located in the altered sections is lowered to 10-12 porosity units (Fig. 9). Other examples can be seen in Figs. 10 and 11. This drop is not definitely established because of the presence of gas (no interconnected porosity in shales). Again, if one or two neutron porosity reductions are credited to high-temperature effect, the balance must be due to a lowering of hydrogen index in shales. When shales show evidence of clay alteration, one would expect more extensive alteration of interstitial clays in porous and permeable sands, and thus the effect on neutron porosity will be more pronounced.

In summary, the apparent lowering of  $\phi_N$  values vs  $\phi_D$  against the altered sands are probably the result of lowering of the hydrogen indices of interstitial clays caused by hydrothermal alteration.

#### IV. USE OF HISTOGRAMS AND SPIDERWEB DIAGRAMS

Manual identification of various zones may be done through the construction of histograms and spiderweb diagrams. Log data may be zoned for statistical studies. Histograms constructed in this study were based on the use of unzoned data. This approach was taken to examine the raw data.

Typical histograms for Well M-42 are shown in Figs. 12 to 15. Using the mean values from the frequency distribution plots, spiderweb diagrams were constructed to examine the characteristic shape for altered and unaltered formations.

Figures 16 and 17 show the characteristic shape of such diagrams in the altered and unaltered sections of Wells M-42 and M-19, respectively. Altered

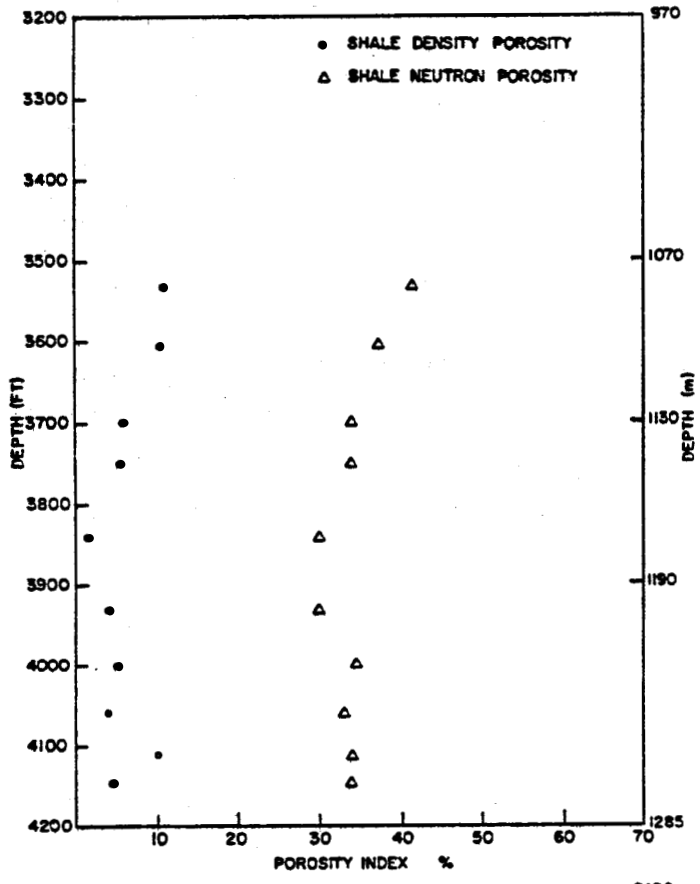
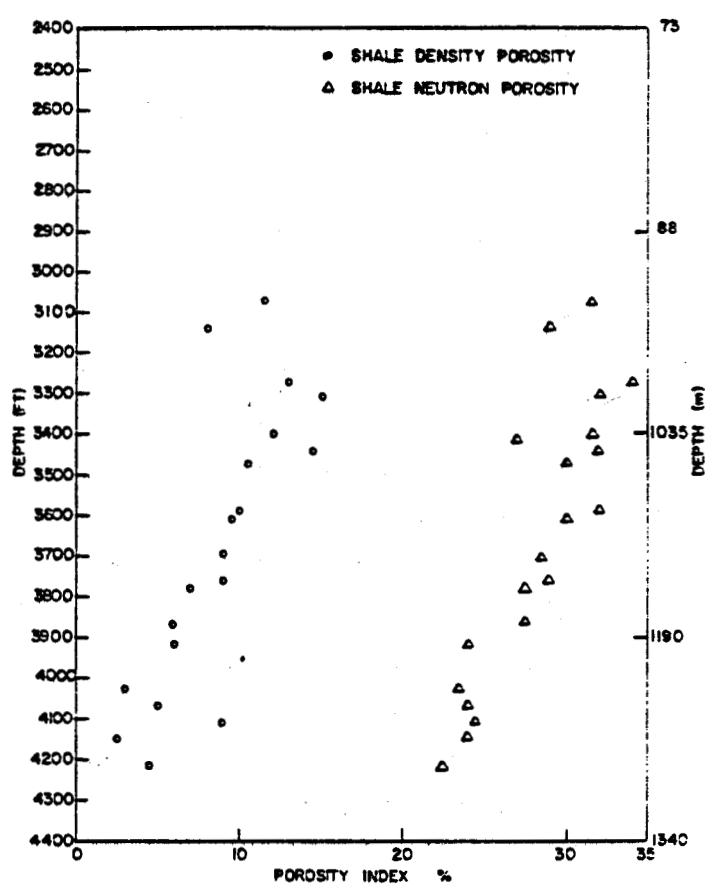


Fig. 10.  
CNL and FDC porosity differences in shales, Well M-29.

Fig. 11.  
CNL and FDC porosity differences in shales, Well M-27.



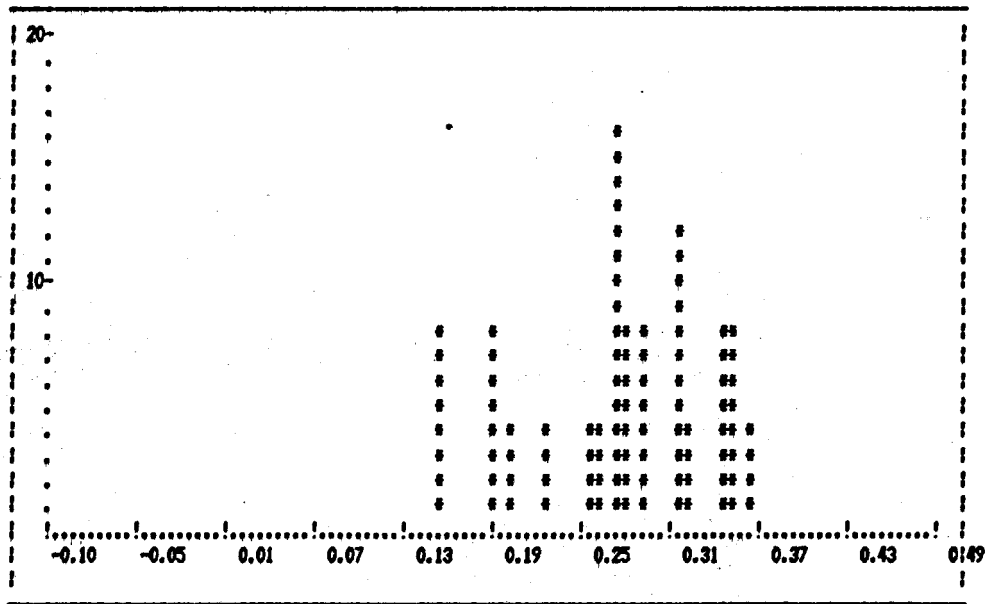


Fig. 12.

Histogram of  $\phi_D$  for an unaltered section of Well M-42.

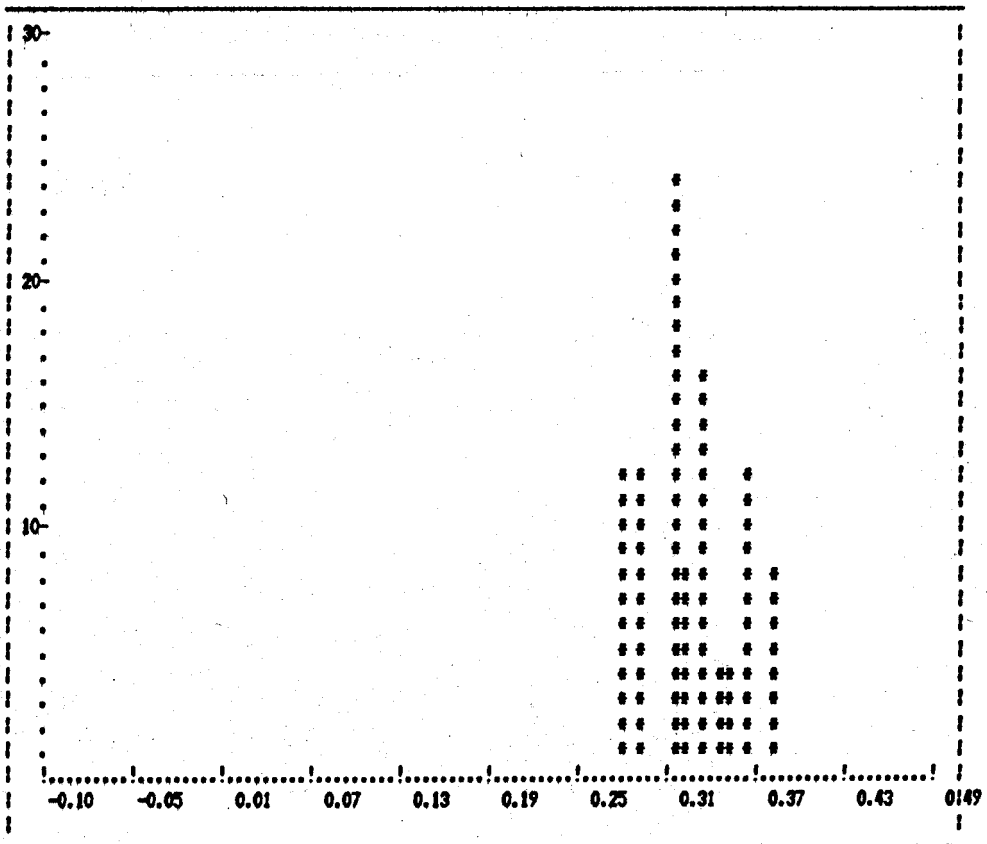


Fig. 13.

Histogram of  $\phi_N$  for an unaltered section of Well M-42.

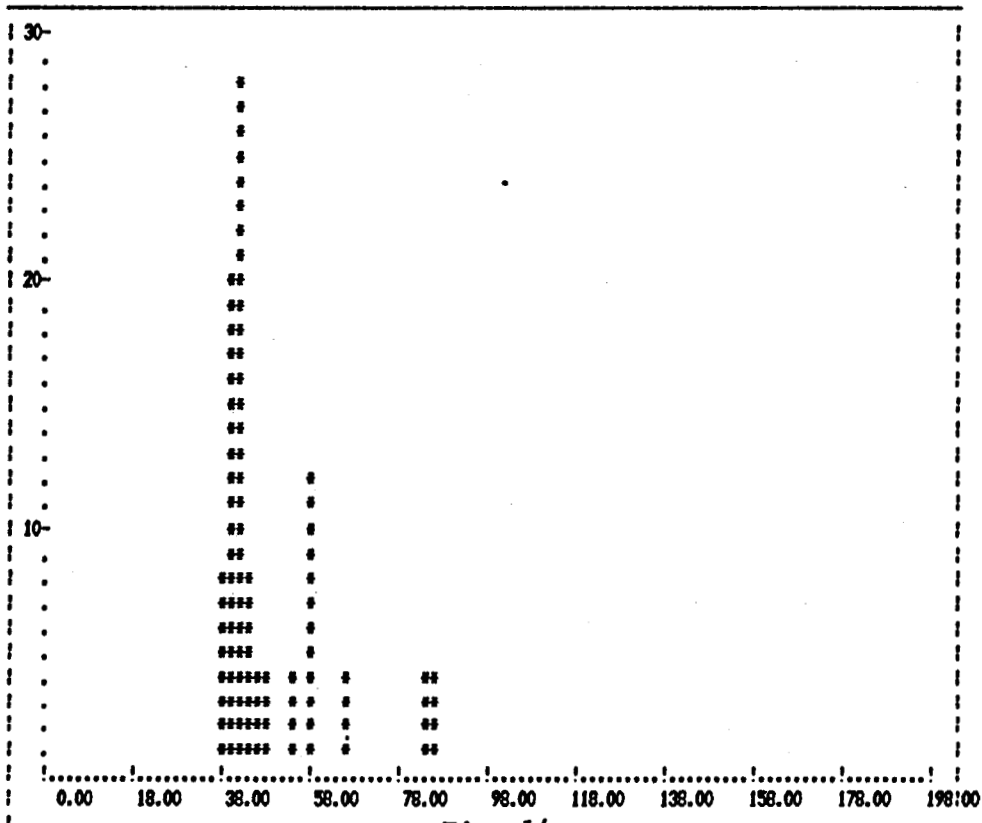


Fig. 14.

Histogram of GR for an unaltered section of Well M-42.

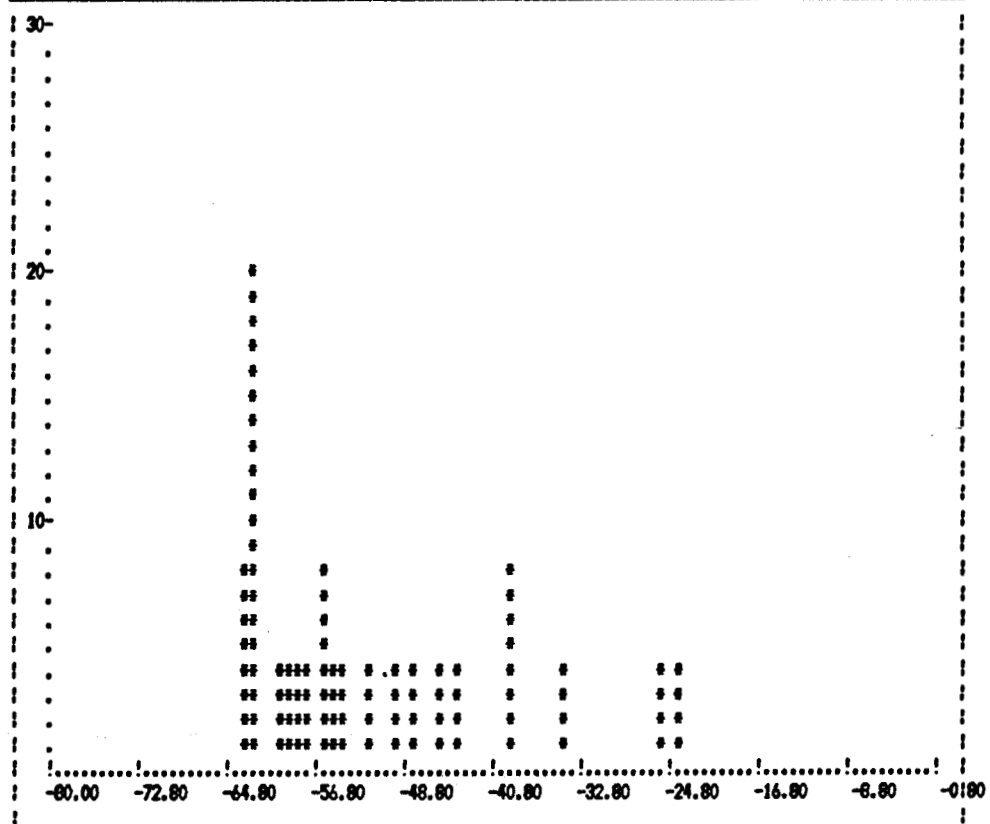


Fig. 15.

Histogram of SP for an unaltered section of Well M-42.

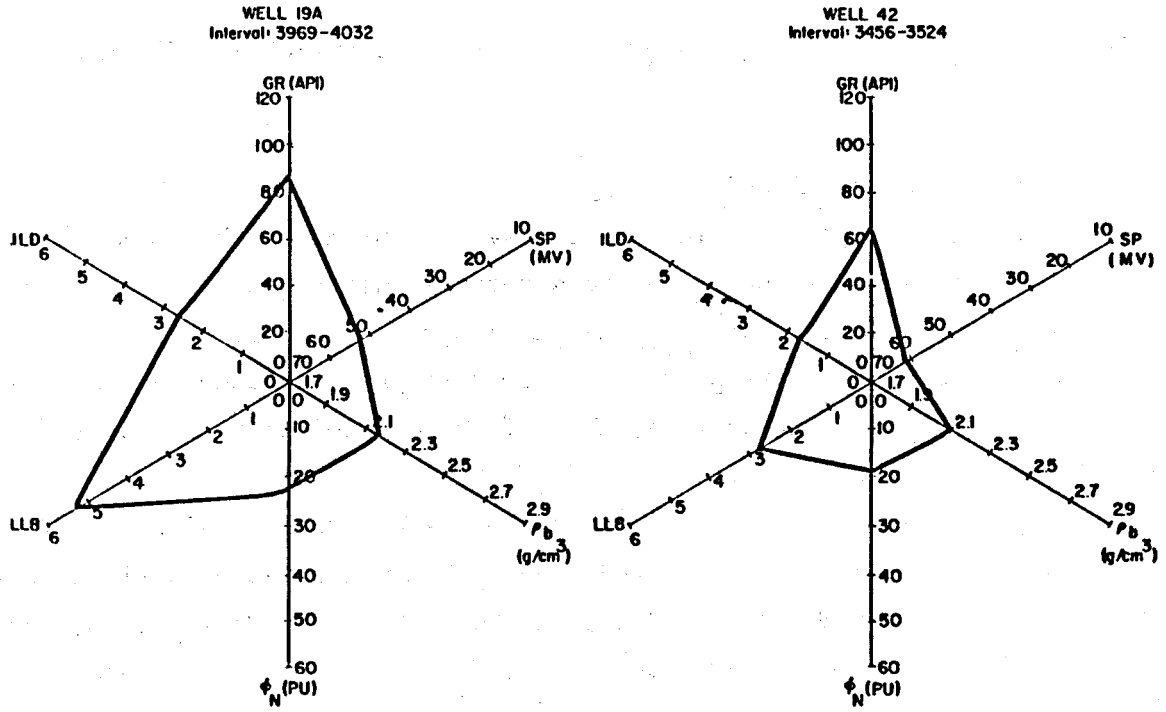


Fig. 16.

Typical spiderweb diagrams in altered zones.

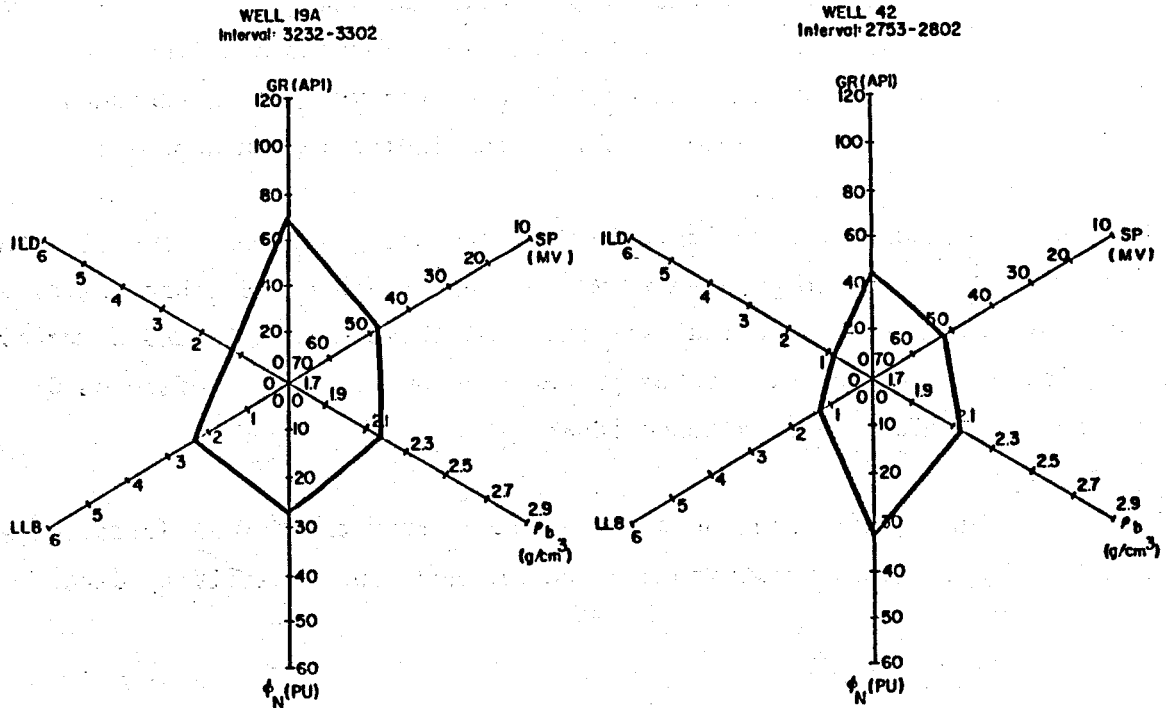


Fig. 17.

Typical spiderweb diagrams in unaltered zones.

zones are characterized by high values of resistivities (SP,  $\rho_b$ , GR) and low values of  $\phi_N$ .

#### V. ESTIMATION OF $Q_v$ -DEPTH PROFILE

Conventional methods of estimating the shale content of the formation will not serve the purpose of identifying hydrothermally altered zones. Fig. 18 shows a typical plot where the  $v_{\text{shale}}$  values computed for Well M-29 from x-ray, SP, and  $\phi_N - \phi_D$  cross plots are plotted for comparison. The computed values do not indicate any trend. Furthermore, the values computed from the three techniques are quite different.

The computed values from  $\phi_N - \phi_D$  cross plots are zero because of the low-hydrogen indices encountered in altered zones. Meanwhile, the SP derived shales content are about 0.2 indicating the lowering of SP deflection in low-permeability shaly sands that have not been completely affected by hydrothermal fluids. While both the SP and  $\phi_N - \phi_D$  cross-plot derived values of shales content are influenced by the changes in the exchange capacity of clays and their dehydration, the x-ray derived values are high and indicate insensitivity to hydrothermal alteration. This is because of the continuous presence of potassium or other radioactive elements that will not change because of hydrothermal activities. In fact, as mentioned earlier, indications from the spiderweb diagrams are that some radioactive elements may have been added to the system from the invading hydrothermal fluids indicating an apparent increase in the shale content.

The above methods are unreliable in distinguishing altered and unaltered clays, so we approached the problem from a different angle. Because the alteration of clays changes the chemical structure of these materials and a net drop in the cation exchange capacity takes place, a computed depth profile of  $Q_v$  will aid in identification of altered zones.

##### A. Procedure

The following equation can be derived for  $Q_v$  from the Waxman-Smiths equation written for the deep formation and the flushed zone resistivity data:

$$Q_v = \frac{C_w - C_{mf} \cdot \frac{R_{xo}}{R_t}}{[B]_{cw} - [B]_{mf} \cdot \frac{R_{xo}}{R_t}} ; \quad (6)$$



$$C_t = (C_w + [B]_{cw} \cdot Q_v) \cdot F^{*-1} \text{ (deep zone)} \quad ; \quad (7)$$

$$C_{xo} = (C_{mf} + [B]_{mf} \cdot Q_v) \cdot F^{*-1} \text{ (flushed zone)} \quad (8)$$

In this derivation, it is assumed that the  $Q_v$  and the porosity of the formations are uniform laterally.

Dual-Induction Laterolog data may be used to estimate  $R_{xo}/R_t$  and, from a knowledge of  $C_w$  and  $C_{mf}$ ,  $Q_v$ -depth profile may be computed.

In practice, however, estimates of  $C_w$  and reservoir temperature may not be available. For a clean rock saturated with brine, the  $C_w$  may be obtained from the SP log.

The SP reading opposite a permeable bed is related to the activities of mud filtrate and formation water. For brine salinities less than 60000 ppm, the activity ratio may be replaced by resistivity ratio and the following equation is used for SP:

$$SP = -K \log \frac{(R_{mf})_e}{(R_w)_e} = -K \log \frac{(C_w)_e}{(C_{mf})_e} \quad , \quad (9)$$

where

$$K = 64.25 + 0.2394 T. \quad (10)$$

The relationship between SP and  $Q_v$  of the sand and adjacent shale was discussed before and may be represented by the following equation

$$\Delta E_c = (E_m)_{sh} - (E_m)_s \quad , \quad (11)$$

where  $(E_m)_{sh}$  and  $(E_m)_s$  are from Eqs. (4) and (5).

Addition of this equation introduces a new unknown,  $(Q_v)_{sh}$ . But it also provides an extra equation should an iterative method be employed.

#### B. Application to the Cerro Prieto Wells

As mentioned earlier, abnormally high values of SP are observed opposite the hydrothermally altered permeable sands. If one assumes the  $Q_v$  of the interstitial clays is zero in such sands, from Eq. (6) we may write

$$\frac{C_w}{C_{mf}} = \frac{R_{xo}}{R_t} \quad (12)$$

From this equation and Eq. (9), an estimation of formation temperature in the vicinity of the wellbore and at the time of logging may be obtained:

$$T = 0.555[-483 - SP/(1.33 \log(.85 R_{mf}/R_{we}))] \quad (13)$$

where

$$R_{we} = [.24 + \log(R_w + .58)]/.69$$

If the computed temperature is equal to or higher than the bottom-hole temperature reported on the log heading, the computations will proceed. Otherwise, estimates of  $R_{mf}$  or  $R_{xo}/R_t$  are adjusted slightly to obtain a reasonable value of temperature.

The unreliability of  $R_{mf}$  data stems from the environmental effects that the mud or mud filtrate may have undergone in the extreme conditions of the borehole. The  $R_{xo}/R_t$  data are subject to uncertainties associated with the depth correlation of recorded resistivities, inadequacy of the Dual-Induction-Laterolog charts to cover certain ranges of resistivities, and improperly corrected resistivities.

Once an acceptable temperature is estimated, the recorded SP is corrected to 25°C using the following equation:

$$(SP)_{25^\circ C} = (SP)_T \cdot \frac{273}{273 + T} \quad (14)$$

Using  $(Q_v)_s = 0$ , an iterative process is used to solve Eq. (11) and to obtain  $(Q_v)_{sh}$ . The optimum  $(Q_v)_{sh}$  is selected as the one resulting in the minimum difference between  $(SP)_{25^\circ C}$  and  $\Delta E_c$  (less than 3 mv).

The  $C_w$  obtained for the deep sand is assumed to be the upper limit of the formation fluid conductivity for all sands at shallower depths. The lower limit of  $C_w$  for such sands is obtained from the corresponding SP data (Eq. 9). Formation temperature for shallower sands are assumed to vary between an upper limit corresponding to the temperature obtained for the deep sand to a lower limit obtained from linear interpolation of wellbore temperature data.

For all of these combinations of T and  $C_w$ , Eq. (6) is used to estimate  $(Q_v)_s$ . Then  $(Q_v)_{sh}$  is obtained from a trial-and-error approach on Eq. (11). Acceptable answers are selected as the ones resulting in positive values for  $(Q_v)_s$  and  $(Q_v)_{sh}$ .

Computed values of  $(Q_v)_s$  and  $(Q_v)_{sh}$  for Wells M-25 and M-30 at selected depths are shown in Figs. 19 and 20. In both graphs, a lowering of  $(Q_v)_s$  with depth is seen at the two extremes of  $R_w$  while  $(Q_v)_{sh}$  is relatively constant. The computed  $(Q_v)_s$  are in the acceptable range of analytical  $Q_v$ 's measured for shaly sands as reported by Waxman and Smits.<sup>3</sup>

Unfortunately, no analytical measurements of  $(Q_v)_s$  on the core samples from the Cerro Prieto field have been reported. But the computed values are in accordance with the x-ray diffraction data of Elders et al.

## VI. BEHAVIOR OF FOUR-ARM CALIPER AND DIPMETER

One of the important questions raised about any geothermal well is the existence of fractures intersecting the wells. Unfortunately, complete suites of well logs have not been run on the Cerro Prieto wells. Limited time is available for the logging program while the holes are building up temperature after a precooled condition.

In some rare instances where some sonic logs have been run, a comparison of  $\phi_s$  with  $\phi_D$  shows the possibility of microfractures, in the form of secondary porosities (Fig. 21). But no evidence of extensive fractures on the sonic log has been acquired on the limited data examined.

One indication of the presence of fractures intersecting the wellbore is a reversal on the relative position of deep induction log and a shallow investigating resistivity log opposite shales. This condition has been observed in some wells and we made an effort to explain the cause.

A careful examination of the well logs indicates that where such reversals occur, the four-arm caliper logs (if available) do not substantiate the existence of fractures. In the presence of fractures, one expects to see a difference between the magnitude of the hole size recorded by the one-arm caliper and the four-arm caliper.

To further verify this finding, the Dipmeter data (when available) were scrutinized. It was noted that the reversal observed in resistivity logs corresponds to sections indicating formation dip angles larger than  $10^\circ$  to  $15^\circ$ .

As discussed by Cox,<sup>8</sup> in the presence of dipping shales, the resistivities recorded by the deep induction log may indeed be higher than that obtained by a shallow investigating tool. This is because of the difference in the methods of measurement. The deep induction surveys the component of formation

resistivity normal to the hole axis while the short normal and laterolog 8 readings are affected by resistivities in both the horizontal and vertical direction.

In structurally flat shales, the shallow investigating resistivities are ordinarily equal to or larger than the deep induction response. But, as the formation dip increases, the induction log reads higher resistivities while the shallow investigating tool response remains unchanged, and the separation will decrease and even reverse sign. A few examples are shown in Figs. 22 to 24. This condition exists on well logs corresponding to the eastern portion of the field where reservoir dip has been confirmed by other geophysical means (Fig. 25).

## VII. SUMMARY AND CONCLUSIONS

Quantification of well log data is an art requiring not only the correct equations and formulas, but also an understanding of the geology, geophysics, and every piece of reservoir data available to a log analyst. For the Cerro Prieto geothermal field, the task of identifying mineral assemblages with depth using well log data is presently impractical because of inadequate logs and insufficient calibration data. The problem of inadequate logs will be resolved when high-temperature tools become available to the industry. The preliminary work on obtaining calibration data started by the Geothermal Log Interpretation Program (GLIP) must continue. This study shows that certain procedures may be applied to the existing well logs to obtain a description of potentially producing zones.

Careful review of well logs indicates that certain patterns are obtained if one constructs spiderweb diagrams from the histograms of various well logs. These patterns indicate changes in resistivity curves, neutron porosities, and the SP log, which can all be related to the characteristics of interstitial clays.

We have relied on the petrographic analysis of the Cerro Prieto cores as published by researchers at the University of California in Riverside. Delineation of various mineral groups analyzed by x-ray diffraction is impractical from our current well log information. But the behavior of clays changing from the low-temperature type in shallow sediments to the high-temperature types in the altered zones is tractable on the well logs.

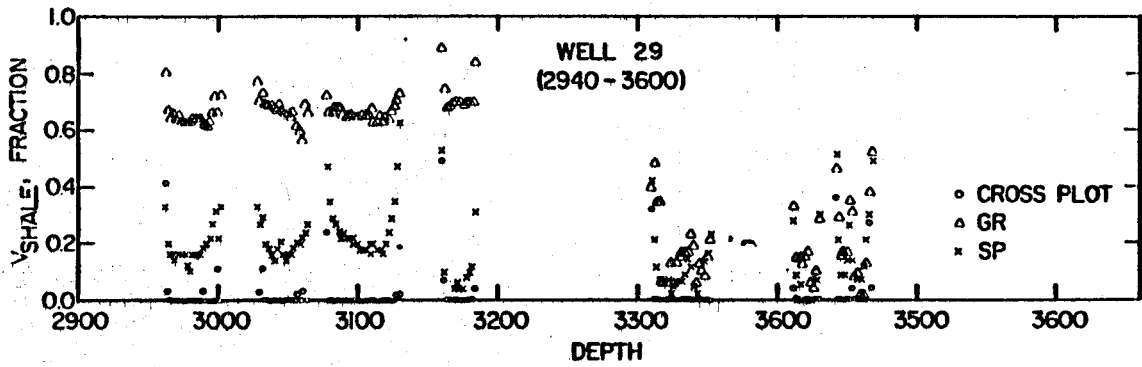


Fig. 18.

Typical  $V_{shale}$  calculated from gamma ray, SP, and  $\phi_N - \phi_D$  cross plots.

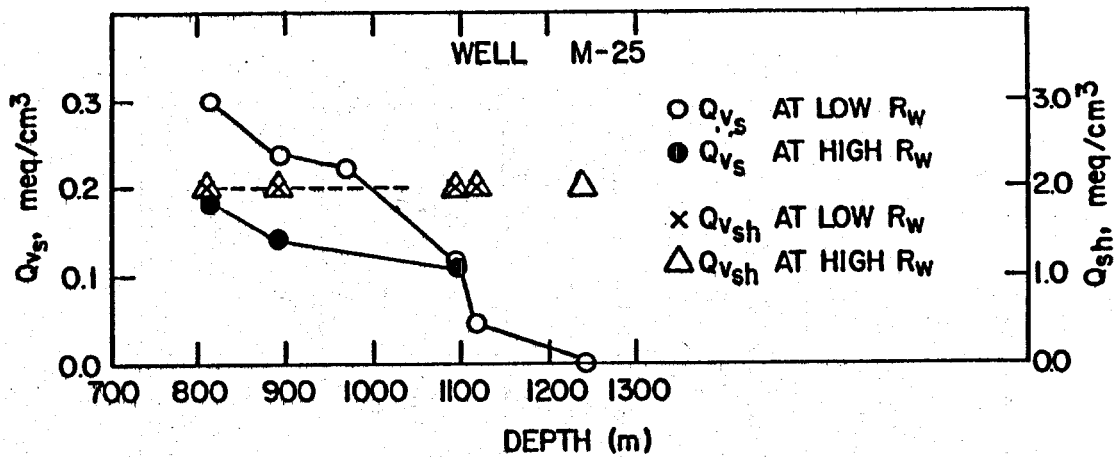


Fig. 19.

Computed  $Q_{vs}$  and  $Q_{vsh}$  with depth, Well M-25.

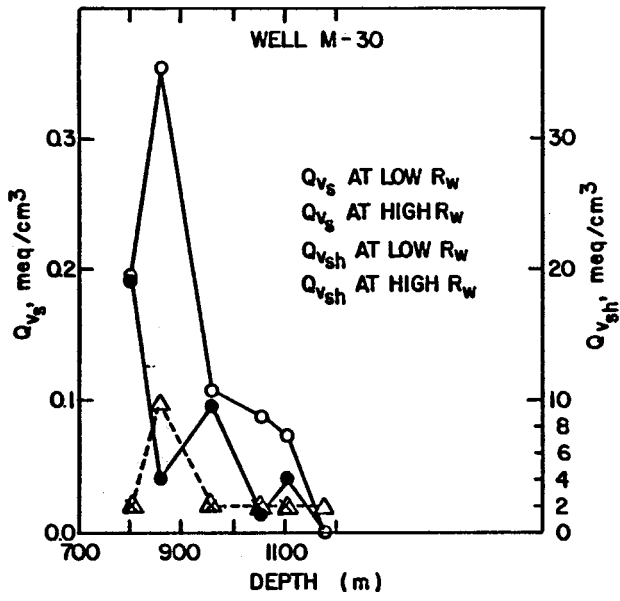


Fig. 20.

Computed  $Q_{v_s}$  and  $Q_{v_{sh}}$  with depth, Well, M-30.

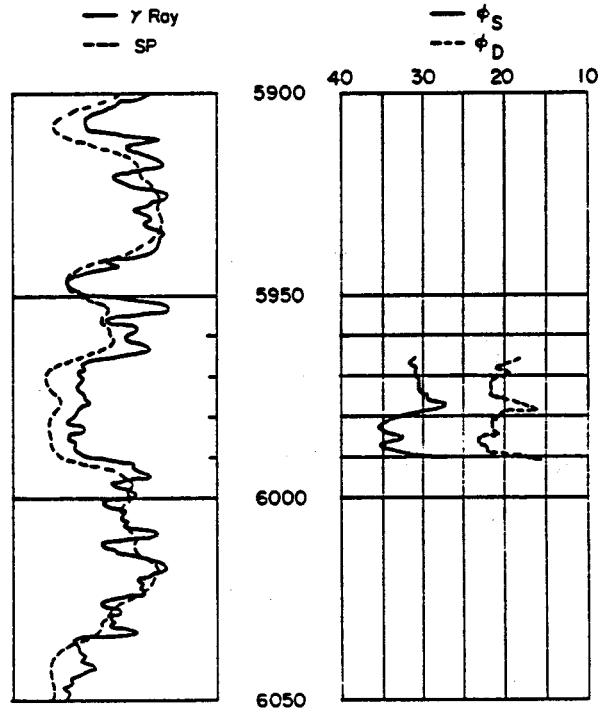


Fig. 21.

Comparison of sonic and density porosities, Well-110.

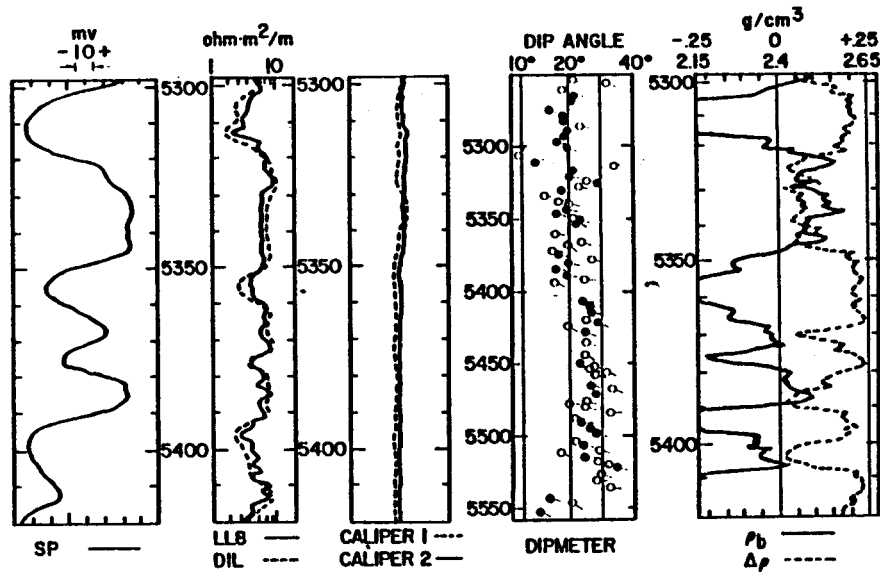


Fig. 22.

Effect of formation dip on the behavior of DIL and LL8, Well M-110.

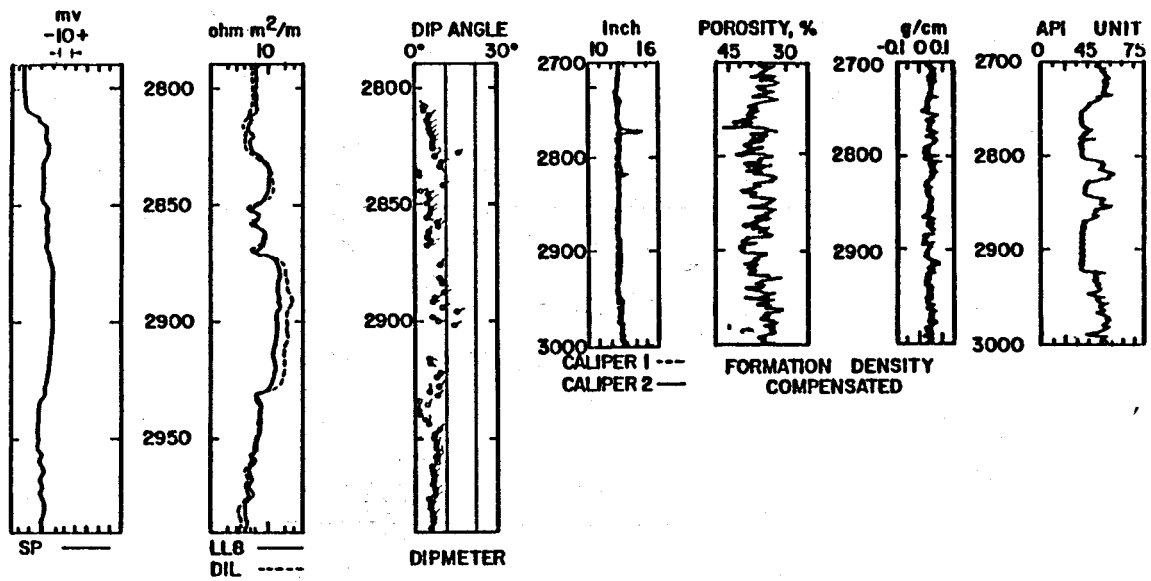


Fig. 23.

Effect of formation dip on the behavior of DIL and LL8, Well M-149.

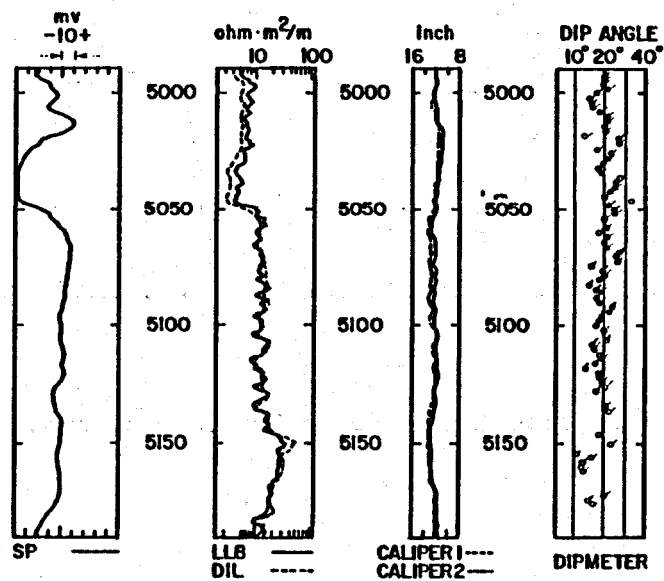


Fig. 24.

Effect of formation dip on the behavior of deep induction log and Laterolog 8, Well M-123.

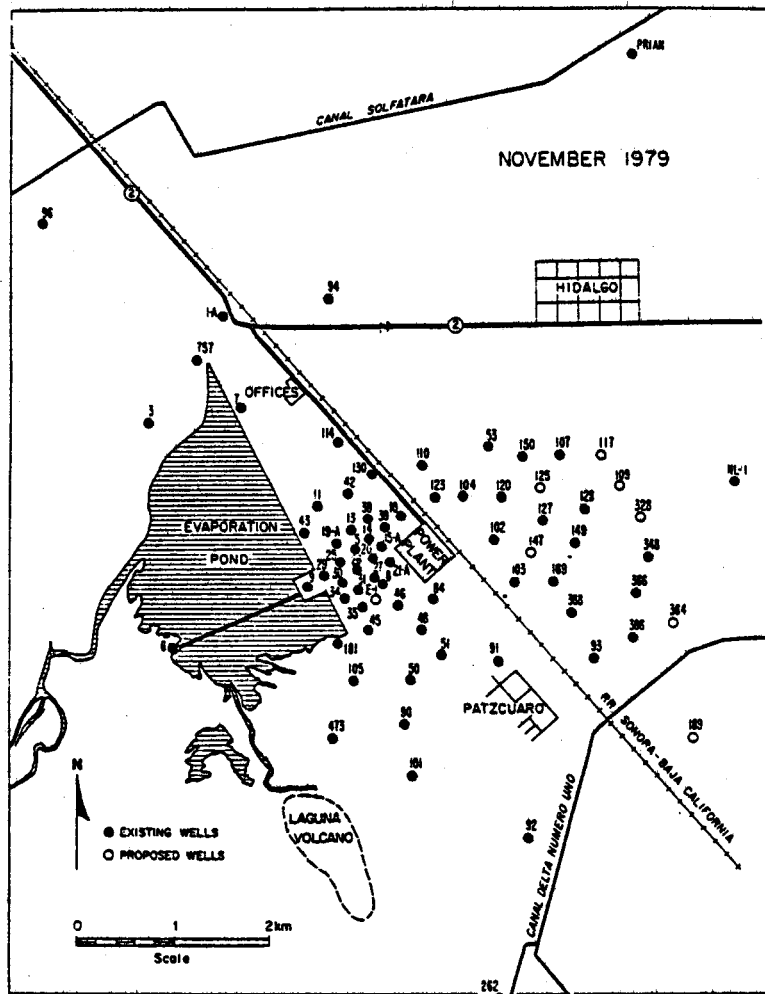


Fig. 25.  
Well location in the Cerro Prieto geothermal field.



In this study, a method for quantification of clay property changes with depth is suggested. The method computes the  $Q_v$ -depth profile to identify the onset of hydrothermally altered zones.

From the examination of existing logs, indications are that the hydrothermally altered sediments of the Cerro Prieto reservoir may contain secondary porosity as indicated by sonic logs. However, no extensive fracturing intersecting the wells has been identified.

#### ACKNOWLEDGMENTS

This study was supported by the Geothermal Log Interpretation Program (GLIP) of the Los Alamos National Laboratory. Mark Mathews, the director of GLIP, supervised the progress of the study with great interest and much encouragement. Portions of this study were presented in two technical papers<sup>9-10</sup> with the permission of the Los Alamos National Laboratory. We wish to thank Marcello Lippmann from Lawrence Berkeley Laboratory for his assistance in obtaining well log data. Many students at the University of Southern California actively participated in various aspects of this study. In particular, we wish to thank Ron Dorovi and Mehran Ramazani, and Maria Vargas for her superb drafting.

#### REFERENCES

1. Elders, W.A., Hoagland, J.R., Olson, E.R., McDowell, S.D., and Collier, P., "A Comprehensive Study of Samples from Geothermal Reservoirs: Petrology and Light Stable Isotope Geochemistry of Twenty-Three Wells in the Cerro Prieto Geothermal Field, Baja California, Mexico," University of California, Riverside, Report UCR/IGPP 78/26 (December 1978).
2. Johnson, W.L., and Linke, W.A., "Some Practical Applications to Improve Formation Evaluation of Sandstones in Mackenzie Delta," paper presented at the 6th Formation Evaluation Symposium of Canadian Well Logging Society in Calgary, Canada (October 24-26, 1977).
3. Waxman, M.H., and Smits, L.J.H., "Electrical Conductivities in Oil-Bearing Sands," SPEJ (June 1968).
4. Uco, H., "Temperature Dependence of the Electrical Resistivity of Aqueous Salt Solutions and Solution-Saturated Porous Rocks," Ph.D. Dissertation, Univ. of So. California (December 1979).
5. Hill, H.J., and Milburn, J.D., "Effect of Clay and Water Salinity on Electrochemical Behavior of Reservoir Rock," Trans. AIME (1956) pp. 65-72.

6. Smits, L.J.M., "SP Log Interpretation in Shaly Sands," SPEJ (June 1968) 123-126.
7. Thomas, E.C., "The Determination of  $Q_v$  from Membrane Potential Measurements on Shaly Sands," SPE 5505, paper presented at the 1975 Fall Meeting of SPE, Dallas, Texas (September 28-October 1, 1975).
8. Cox, J.W., "The High Resolution Dipmeter Reveals Dip-Related Borehole and Formation Characteristics," Trans. SPWLA (May 3-6, 1970).
9. Ershaghi, I., Ghaemian, S., and Mathews, M., "Detection of Hydrothermal Alterations in a Sedimentary Type Geothermal Reservoir," SPE 9499, paper presented at SPE Fall Meeting, Dallas, Texas (September 21-24, 1980).
10. Ershaghi, I., and Ghaemian, S., "Estimation of  $Q_v$  Profile in a Sedimentary Type Geothermal Reservoir," SPE 9927, paper presented at the 1981 California Regional Meeting of SPE, Bakersfield, California (March 25-26, 1981).